Author Manuscript

Author Manuscript

Author Manuscript

Author Manuscript

HHS Public Access

Author manuscript

Biol Psychiatry. Author manuscript; available in PMC 2024 November 15.

Published in final edited form as:

Biol Psychiatry. 2023 November 15; 94(10): 769–779. doi:10.1016/j.biopsych.2023.02.993.

Genetic ablation of *GIGYF1*, associated with autism, causes behavioral and neurodevelopmental defects in zebrafish and mice

Zijiao Ding[1,2,12], **Guiyang Huang**[3,12], **Tianyun Wang**[4,5,6,12], **Weicheng Duan**[1], **Hua Li**[7], **Yirong Wang**[7], **Huiting Jia**[1], **Ziqian Yang**[1], **Kang Wang**[1], **Xufeng Chu**[1], **Evangeline C Kurtz-Nelson**[8], **Kaitlyn Ahlers**[8,†], **Rachel K Earl**[8], **Yunyun Han**[3], **Pamela Feliciano**[9], **Wendy K Chung**[9,10], **Evan E Eichler**[6,11], **Man Jiang**[7,*], **Bo Xiong**[1,*]

[1]Department of Forensic Medicine, Tongji Medical College, Huazhong University of Science and Technology, Wuhan 430030, Hubei, China

[2]Department of Pathology, School of Basic Medicine, Anhui Medical University, Hefei, Anhui 230032, China

[3]Department of Neurobiology, School of Basic Medicine, Tongji Medical College, Huazhong University of Science and Technology, Wuhan 430030, Hubei, China

[4]Department of Medical Genetics, Center for Medical Genetics, Peking University Health Science Center, Beijing 100191, China

[5]Neuroscience Research Institute, Peking University; Key Laboratory for Neuroscience, Ministry of Education of China & National Health Commission of China, Beijing 100191, China

[6]Department of Genome Sciences, University of Washington School of Medicine, Seattle, WA 98195, USA.

[7]Department of Physiology, School of Basic Medicine, Tongji Medical College, Huazhong University of Science and Technology, Wuhan 430030, Hubei, China

[8]Department of Psychiatry & Behavioral Sciences, University of Washington, Seattle, WA 98195, USA

[9]The Simons Foundation, New York, NY 10010, USA.

[10]Department of Pediatrics, Columbia University, New York, NY 10032, USA

[11]Howard Hughes Medical Institute, University of Washington, Seattle, WA 98195, USA.

[*]Correspondence to: bxiong@hust.edu.cn (B.X.), manjiang@hust.edu.cn (M.J.).

[†]Present address: Department of Psychiatry, Geisel School of Medicine at Dartmouth, Dartmouth Hitchcock Medical Center, Lebanon, NH, USA

Disclosures

E.E.E. is on the scientific advisory board of Variant Bio, Inc. All other authors report no biomedical financial interests or potential conflicts of interest.

Publisher's Disclaimer: This is a PDF file of an unedited manuscript that has been accepted for publication. As a service to our customers we are providing this early version of the manuscript. The manuscript will undergo copyediting, typesetting, and review of the resulting proof before it is published in its final form. Please note that during the production process errors may be discovered which could affect the content, and all legal disclaimers that apply to the journal pertain.

Author Manuscript Author Manuscript Author Manuscript Author Manuscript

[12]These authors contributed equally

Abstract

Background—Autism spectrum disorder (ASD) is characterized by deficits in social communication and restricted or repetitive behaviors. Due to the extremely high genetic and phenotypic heterogeneity, it is critical to pinpoint the genetic factors for the understanding of the pathology of these disorders.

Methods—We analyzed the exomes generated by the SPARK project and performed a meta-analysis with previous data. We then generated a zebrafish knockout model and three mouse *Gigyf1* knockout models to examine the function of *GIGYF1* in neurodevelopment and behavior. Finally, we performed whole tissue and single-nuclei transcriptome analysis to explore the molecular and cellular function of *GIGYF1*.

Results—*GIGYF1* variants are significantly associated with various NDD phenotypes including autism, global developmental delay, intellectual disability, sleep disturbance. Loss of *GIGYF1* causes similar behavioral effects in zebrafish and mice, including elevated levels of anxiety and reduced social engagements, which is reminiscent of the behavioral deficits in human patients carrying *GIGYF1* mutations. Moreover, excitatory neuron-specific *Gigyf1* knockout mice recapitulate the increased repetitive behaviors and impaired social memory, suggesting a crucial role of *Gigyf1* in excitatory neurons, which correlates with the observations in single nuclei RNAseq. We also identified a series of downstream target genes of *GIGYF1* that affects many aspects of the nervous system especially synaptic transmission.

Conclusion—*De novo* variants (DNVs) of *GIGYF1* are associated with NDDs including ASD. *GIGYF1* is involved in neurodevelopment and animal behavior, potentially through regulating hippocampal CA2 neuronal numbers and disturbing synaptic transmission.

Keywords

GIGYF1 ; Autism spectrum disorder; Developmental delay; Neurodevelopmental disorder; Social behavior; zebrafish; mouse

Introduction

Autism spectrum disorder is a group of the neurodevelopmental disorder that is defined by social communication deficits and repetitive or stereotyped behaviors of early onset (1). In addition, some of the individuals with ASD also exhibit one or more co-occurring symptoms such as intellectual disability, sensory issues, sleep disorders, and gastrointestinal dysfunction (2, 3). The global prevalence of ASD worldwide is about 1%−2%(4), and the number of individuals diagnosed has been increased steadily over the past 20 years(5). Genetic factors are major causes of ASD, with extremely high genetic heterogeneity and complex genetic architecture (6, 7). Recently, large-scale genetic studies have identified multiple risk genes and highlighted the contributions of DNVs to ASD (8–10).

There is emerging evidence suggesting that DNVs in *GIGYF1* are associated with ASD and related NDDs. Initially, three *de novo* likely gene disruptive (dnLGD, including stop

Author Manuscript Author Manuscript Author Manuscript Author Manuscript

gained, frameshift or splice mutations) variants were identified by exome sequencing of 2,508 autism families from the Simons Simplex Collection (SSC) (11). Another dnLGD variant was identified in 465 ASD trios by the SPARK pilot project (12). Furthermore, one dnLGD variant were identified in 3,625 trios by the Autism Sequencing Consortium (ASC) (13). Moreover, in a large cohort of developmental disorders (DD), eight dnLGD variants and six *de novo* missense (dnMIS) variants were identified from 31,058 DD parent-offspring trios (14). In this study, we identified seven additional DNVs of *GIGYF1* from 7,015 autism exome trios, and performed a meta-analysis with previous studies to show that disruptions of *GIGYF1* are associated with NDD phenotypes especially for autism.

GIGYF1 was originally identified as a binding partner to the tandem proline-rich region in the N-terminus of Grb10 in a yeast two-hybrid screening, and it was proposed to activate IGF-1 signaling. (15). It was then found to repress target mRNA expression through interacting with 4EHP, which competes eIF4E to bind to the 5’ cap structure of specific mRNAs (16, 17). Moreover, GIGYF1 is reported to be involved in translation-coupled-mRNA-decay through the binding with 4EHP (18). In *Drosophila*, *gyf* (homolog of *GIGYF1* and *GIGYF2*) was found to regulate autophagy (19). The null allele *gyf* flies exhibited shortened life span and impaired motor ability. Nevertheless, the role of *GIGYF1* in nervous system development remains poorly understood. Here, we generated zebrafish and mouse models of *GIGYF1* and found that the phenotypes observed in these models correlate well with the symptoms of patients carrying *GIGYF1* variants, establishing a causative relationship between *GIGFY1* mutations and neurodevelopmental defects.

Methods and Materials

Animal models

All animals were kept at standard temperature with controlled circadian cycle. The zebrafish mutant alleles were generated using CRISPR/Cas9 genome editing technology as previously described (20). *Gigyf1* conditional knockout (cKO) mice were generated using the CRISPR/CAS9 system to flank the 10th-24th exons by loxP sites. Constitutive Gigyf1 knockout mice were generated by crossing cKO with CMV-Cre. All animal experiments were approved by the Animal Care and Use Committee of the animal core facility at Huazhong University of Science and Technology.

Behavioral tests

All behavioral tests were performed using animals of the same age, gender, raising conditions with littermate control. Zebrafish larval adaptation assay, novel tank test, shoaling test, social behavior test, and mirror test were performed as previously described. Mice open field test, elevated-plus maze, novel object recognition test, grooming test, marble burying test, T-maze, three-chamber sociability test and fear conditioning test were performed at age of 6–10 weeks according to standard protocols.

Transcriptomics

For zebrafish, heads of 4.3 days post fertilization (dpf) larvae were dissected out and total RNA were extracted for transcriptomic analyses. For mice, the cortex and hippocampus

Author Manuscript Author Manuscript Author Manuscript Author Manuscript

of P0 mice were dissected and used for bulk RNA sequencing. For single nuclei RNA sequencing (snRNA-seq), hippocampi dissected from 6-week old mice were used, followed by library preparation using 10X Genomics pipeline. Sequencing was performed with Illumina NovaSeq6000.

Detailed methods, statistics statement, data and code availability is in the supplementary information.

Results

Excess of *de novo GIGYF1* variants in NDD patients

We first identified seven DNVs (P1-P7, three dnLGD and four dnMIS variants) in *GIGYF1* from exome sequencing of 7,015 trios with autism diagnosis from the SPARK project (21) , and then integrated with another 19 DNVs (P8-P26, 13 dnLGD and 6 dnMIS) from previously published cohorts with a primary diagnosis of ASD or DD (Supplementary table 1) (11–14, 22). Taken together, we assembled a cohort of 26 DNVs in *GIGYF1* from a total of 44,665 unique NDD families (Supplementary table 2). The ratio of DNVs in ASD is ~1.96 fold higher than that in DD cases (0.088% in ASD vs. 0.045% in DD, p = 0.06, one-sided Fisher's exact test) (Figure 1, Supplementary table 1). We re-evaluated the DNV enrichment for all genes using two statistical models: a modified chimpanzee–human divergence model (23) (CH model) and the denovolyzeR (24) model. Both models identified a significant excess of dnLGD variants of *GIGYF1* in NDD: CH model (P_{adj} = 4.62E-14, corrected by 18,946 genes tested) and denovolyzeR (P_{adj} = 2.3E-16, corrected by 19,618 genes tested). These results confirmed the DNVs in *GIGYF1* are significantly associated with NDDs.

Disruption of *GIGYF1* is associated with autism and other NDD phenotypes

We were able to obtain detailed clinical information for 14 probands (P1-P14), whose average age at registration was 9.8 years old (Supplementary table 3). The majority of probands were diagnosed with autism (85.7%, 12/14), and 83.3% (10/12) of cases exhibit behavioral abnormalities, such as social communication disorder, obsessive-compulsive disorder, social anxiety disorder or social phobia. Speech delay and sleep disturbance (e.g., sleep disordered breathing, difficulty to fall asleep, long and frequent naps, or nocturnal incontinence) were commonly co-occurred. Dysmorphic facial features (27.3%, 3/11), such as hypertelorism, wide nasal bridge or cleft palate, are usually seen in patients with DD, but not in autism cases, suggesting that it could be an indicator for more severe phenotypes. In addition, intellectual disability (35.7%, 5/14), motor delay (25%, 3/12), seizures (18.2%, 2/11), ADHD (18.2%, 2/11), hearing abnormalities (16.7%, 2/12), and cardiac anomalies (16.7%, 2/12) are also observed in subsets of the patients (Figure 1B). In summary, a wide range of ASD or NDD phenotypes are present in probands with DNVs in *GIGYF1.*

Generation of zebrafish knockout alleles of *gigyf1*

There are two homologous genes of human *GIGYF1* in zebrafish, namely *gigyf1a* and *gigyf1b* (Supplementary Figure 1A & B). We performed *in situ* hybridization and RT-qPCR to determine the temporal-spatial expression patterns of the two genes and found that they

Author Manuscript Author Manuscript Author Manuscript Author Manuscript

are both maternally and ubiquitously expressed during zygote cleavage, gastrulation and epiboly and enriched in the head regions after 24 hpf (Supplementary Figure 1C & D). We targeted the two genes using the CRISPR/Cas9 system and generated a 16 bp deletion allele for *gigyf1a* and a 4 bp deletion allele for *gigyf1b*, both which introduce frameshifts and early truncations to the corresponding proteins (Figure 2A & B). We further performed sanger sequencing, qPCR and western blot to verify the knockout effect of the mutant (Supplementary Figure 1E–G). We subsequently crossed the homozygous single mutants and obtained homozygous *gigyf1a*; *gigyf1b* double mutant.

Loss of *gigyf1a* and *gigyf1b* leads to developmental defects in zebrafish

To evaluate whether knockout of *gigyf1a* and *gigyf1b* affects zebrafish development, we measured the body length and the distance between the convex tips of the eyes (interorbital distance, which is an indicator of the brain size) (2). The overall embryonic development was not affected in any of the single mutants, except for a mild (~4%, $p = 0.006$) reduction of the interorbital distance in *gigyf1b*$^{-/-}$ (Supplementary Figure 2). However, the body lengths of 4.3-dpf double mutant larvae (~3%, $p < 0.001$) and 3-month adult fish (~9%, $p < 0.001$) were both significantly reduced (Supplementary Figure 3A–D). Moreover, the interorbital distance was further reduced (~10%, $p < 0.001$) in the double mutant compared to *gigyf1b* single mutant (Supplementary Figure 2G, H and 3E, F). We further examined cell proliferation and apoptosis in the head region and observed that cell proliferation was significantly reduced in the double mutants at 3 dpf and 6 dpf, and the apoptosis levels were elevated at 6 dpf (Supplementary Figure 3G, H). The abnormal proliferation and apoptosis levels are potentially contributing to the early embryonic developmental defects.

Loss of *gigyf1a* and *gigyf1b* leads to behavioral defects related to human patient phenotypes

Next, we assessed the behaviors of the mutant. We performed an adaptation assay with repeated dark stimulation using 5-dpf larvae (Supplementary Figure 4A). The initial responses were similar among all genotypes, and the control larvae exhibited gradually reduced responses since the second round of stimulation whereas the *gigyf1a*$^{-/-}$; *gigyf1b*$^{-/-}$ larvae failed to adapt (Supplementary Figure 4 B–G). We then performed behavioral tests in adult fish (Supplementary Figure 5). In the novel tank test, the mutants spent more time in the bottom region (Cohen's $d = -0.9180$, $p = 0.003$) and less time in the middle (Cohen's $d = 0.9973$, $p = 0.002$) or top regions (Cohen's $d = 1.0321$, $p = 0.001$), indicating higher levels of anxiety (Figure 2C). In the mirror test, the mutants tended to move away from the reflection in the mirror (contact: Cohen's $d = 1.7656$, $p < 0.001$; approach: Cohen's $d = 0.1491$, $p = 0.638$; far: Cohen's $d = -2.2554$, $p < 0.001$), indicating reduced aggression levels in the mutants (Figure 2D). In the three-chamber test, the mutants spent less time in the social area compared to controls (left: Cohen's $d = 0.5937$, $p = 0.05$; middle: Cohen's $d = -0.9309$, $p = 0.003$; right: Cohen's $d = -0.7761$, $p = 0.013$), indicating attenuated social preference (Figure 2E). Moreover, the frequency for the fish to enter into each zone (left: Cohen's $d = -0.9298$, $p = 0.003$; middle: Cohen's $d = -1.4640$, $p < 0.001$; right: Cohen's $d = -1.0774$, $p = 0.001$) as well as the average velocity (Cohen's $d = -1.4722$, $p < 0.001$) were increased in the mutants, again suggesting elevated anxiety levels (Figure 2E). Finally, in the shoaling test, the average distance among the mutants is significantly higher (Cohen's d =

Author Manuscript Author Manuscript Author Manuscript Author Manuscript

−1.5669, $p < 0.001$), indicating impaired social interactions (Figure 2F). In summary, loss of *gigyf1a* and *gigyf1b* in zebrafish led to defects in adaptation, aggression, anxiety and social interaction behaviors.

Heterozygous knockout of mouse *Gigyf1* results in repetitive behavior and social memory deficits

To examine whether *GIGYF1* plays an evolutionarily conserved role, we also utilized mouse models. At postnatal day 42 (P42), *GIGYF1* was detected at low levels in the spleen, liver and kidney, but at high levels in brain, spinal cord, lung and heart (Figure 3A). Within the P42 brain, *GIGYF1* is expressed in various regions (Figure 3B, Supplementary Figure 6A & B). Moreover, *Gigyf1* mRNA is highly expressed in the nervous system during various embryonic and postnatal periods (Figure 3C & Supplementary Figure 6C).

We flanked the genomic region spanning from the 10^{th} to the 24^{th} exon of *Gigyf1* with loxP sites (Figure 3D). The loxP-flanked *Gigyf1* allele is referred to as a cKO allele. Consequently, we generated constitutive *Gigyf1* KO mice (Figure 3E). The homozygous *Gigyf1* KO mice died shortly after birth, so we utilized the heterozygous *Gigyf1* KO (Het KO) mice for behavioral tests. The *Gigyf1* Het KO mice displayed repetitive behavior with excessive grooming (#Grooming: Cohen's $d = -0.9229$, $p = 0.0394$; Time spent grooming: Cohen's $d = -0.9451$, $p = 0.0353$) (Figure 3F). The locomotion activity was slightly decreased (Cohen's $d = 1.2988$, $p = 0.0031$) without changing the anxiety level in the open field (Figure 3G). We then utilized the three-chamber social interaction assay to evaluate the social behaviors. During the first phase, the sociability of *Gigyf1* Het KO mice was normal (Figure 3H). In the following phase, *Gigyf1* Het KO mice showed a significant deficit in social novelty test (Cohen's $d = 0.8643$, $p = 0.0455$), also referred to as social memory (Figure 3I), suggesting a reduced ability to discriminate novel and familiar conspecifics. We did not detect significant changes in novel object recognition, rearing, marble burying, T maze and elevated plus maze (Figure 3J–N). Therefore, *Gigyf1* Het KO mice displayed an increased repetitive behavior and a decreased social memory, which are characteristics of ASD.

Conditional ablation of *Gigyf1* in excitatory neurons results in repetitive behavior and social memory deficit

Using published datasets of single-cell RNA sequencing, we found that *Gigyf1* was widely expressed in distinct neuron types, especially the glutamatergic and GABAergic neurons in both cortices and hippocampus (Supplementary Figure 7A, B, C). In order to test the functions of *Gigyf1* in different types of neurons, we crossed the *Gigyf1* cKO mice with NEX-Cre and GAD2-Cre mice, respectively, which resulted in knockout of *Gigyf1* in excitatory (e-cKO) or inhibitory neurons (i-CKO) (Figure 4A, Supplementary Figure 7D, E). We performed western blot and qPCR experiments, and confirmed that both the protein and mRNA levels were significantly reduced in the cortical (protein: Cohen's $d = 14.7706$, $p < 0.001$; RNA: Cohen's $d = 36.3422$, $p < 0.001$) and hippocampal regions (protein: Cohen's $d = 2.7161$, $p = 0.0292$; RNA: Cohen's $d = 16.2511$, $p < 0.001$) of the *Gigyf1* e-cKO mice (Figure 4B & C, Supplementary Figure 6D). We then evaluated the behavioral performances of the *Gigyf1*e-cKO and *Gigyf1* i-cKO mice using a series of behavioral tests. The *Gigyf1*

Author Manuscript Author Manuscript Author Manuscript Author Manuscript

e-cKO mice display repetitive behavior with excessive grooming (Cohen's d = −0.7, p = 0.05) (Figure 4D). However, we did not observe significant changes for the *Gigyf1* e-cKO mice in the open filed, novel object recognition, rearing, marble burying and elevated plus maze and fear conditioning tests (Figure 4E & F, Supplementary Figure 6E–F, H–K). In the T maze test, we detected a minor deficit in short-term memory for the *Gigyf1* e-cKO mice (Cohen's d = 0.7804, p = 0.03) (Supplementary Figure 6G). In the three-chamber social interaction assay, the *Gigyf1* e-cKO mice showed a normal sociability (Figure 4G), but displayed a significant deficit in social memory (Cohen's d = 1.3427, p < 0.001) (Figure 4H). Therefore, the *Gigyf1* e-cKO mice phenocopied the increased repetitive behavior and decreased social memory observed in *Gigyf1* Het KO mice.

Interestingly, we observed different behavioral phenotypes in the *Gigyf1* i-cKO mice. These mice displayed reduced grooming behavior (Cohen's d = 1.6758, p = 0.045) (Figure 4I) and elevated anxiety levels (Time in centers: Cohen's d = 1.8695, p = 0.029; Velocity in centers: Cohen's d = −2.5322, p = 0.004) (Figure 4J), which was not observed in the *Gigyf1* e-cKO. We did not detect any significant changes in sociability, social novelty, learning and memory or anxiety (Figure 4K, L, N–Q). However, *Gigyf1* i-cKO mice exhibit a significant impairment in cognitive performance in the novel object recognition test (Cohen's d = 2.2221, p = 0.01) (Figure 4M). In summary, these results showed a neuron type-specific role of *Gigyf1* in mouse behaviors.

GIGYF1 regulates downstream target genes related to neurodevelopment

To explore the molecular mechanisms by which *GIGYF1* regulates neurodevelopment, we performed transcriptomic and proteomic analyses in the 4.3-dpf zebrafish head tissues (Supplementary Figure 8A–F). In total, we identified 1,260 DEGs (461 downregulated and 799 upregulated) from the 20,553 detected genes in the transcriptomics and 286 DEPs (83 downregulated and 203 upregulated) from the 7,848 proteins detected (Supplementary Figure 9A & C, Supplementary Table 4). The correlation between the DEGs and DEPs was poor, potentially due to differences in the detection range, sensitivity and accuracy between the two methods (Supplementary Figure 8G–I). Therefore, we analyzed gene functions for the two lists independently. To explore the functions of the downstream targets, we performed GSEA based on the fold change order for the DEGs and DEPs. The downregulated DEGs were mainly involved in the development of metencephalon, neuron, nerve, dendritic spine and the GABA signaling pathway (Supplementary Figure 9B), whereas the DEPs were mainly involved metabolic pathways and neurodegenerative diseases (Supplementary Figure 9D). We then compared the DEGs/DEPs with the SFARI/DDD gene lists. Interestingly, a subset of the DEGs and DEPs are associated with different subtypes of NDDs (Supplementary Figure 9E). Moreover, we annotated the gene–disease associations for the DEGs and DEPs using the DisGeNET database and found subsets of the DEGs associated with intellectual disabilities, schizophrenia, depression and autism, suggesting that these genes may be involved in the complex neurodevelopmental phenotypes associated with *GIGYF1* variants (Supplementary Figure 9F).

Next, we performed bulk RNA sequencing in the hippocampus and cortex in mice at P0. GSEA enrichment analysis showed a significant downregulation in genes regulating synaptic

Author Manuscript Author Manuscript Author Manuscript Author Manuscript

structure and neurotransmitter transport (Supplementary Figure 10A–D). To explore the conserved molecular pathways, we jointly analyzed the mRNA expression profiles of zebrafish and mouse KO models and identified four up-regulated genes and 14 down-regulated genes (Supplementary Figure 10E & F). The down-regulation of solute carrier family 17 member 7 (*Slc17a7*/*VGLUT1*) and glutamate metabotropic receptor 2 (*Grm2*) suggests potential changes of glutamatergic synapses. Therefore, *GIGYF1* may regulate synaptic transmissions in different species.

GIGYF1 alters the proportion of CA2 glutamatergic neurons

To further explore the neural mechanisms underlying the observed phenotypes, we performed immunohistochemistry on the hippocampus. The overall hippocampal architecture was normal in the *Gigyf1* Het KO mice (Supplementary Figure 11A & B). The density of NeuN-positive neurons in CA2 area was significantly increased (Cohen's $d = -1.4422616$, $p = 0.0194$) (Supplementary Figure 11A & B). We also performed immuno-staining for *vGluT2* (vesicular glutamate transporter 2) and *GAD65/67* (glutamic acid decarboxylase 65 or 67-kD isoform). However, no significant change was observed, suggesting a normal synapse density (Supplementary Figure 11C–F).

Next, we performed single-nuclei RNA sequencing (snRNAseq) in the hippocampus to examine the role of *Gigyf1* in different populations of neurons. We analyzed the transcriptomes of 16211 cells (Ctrl:5965 and Het KO:10246), and identified nine major clusters (Figure 5A). We further clustered the neurons into nine subpopulations (Figure 5B & C). Importantly, the *Gigyf1* Het KO mice harbored a higher percentage of *Slc17a7*$^{+}$ (*Vglut1*$^{+}$) excitatory neurons in the CA2-CA3 region (Figure 5D), correlating with the increased neuron density in CA2 region in NeuN-staining. We further explored the transcriptomic changes in the major glutamatergic neurons. The four clusters of neurons shared common up-regulated gene "*Xist*" and down-regulated gene "*Nr3c2*" (Figure 5E). The significantly down-regulated genes are involved in various processes related to neuronal function, including presynaptic and postsynaptic structures, neurotransmitter transport, membrane potential, ion channel and glutamate receptor activity (Figure 5F & G). In the single cell pseudotime trajectory analysis, neurons in CA area and DG area showed distinct differentiation path originating from neuroblasts (Supplementary Figure 12A & B). We further identified the key DEGs of the differentiation node, many of which were also differentially expressed between Ctrl and Het KO groups (Supplementary Figure 12C). These results indicate that haploinsufficiency of *Gigyf1* leads to increased CA2 glutamatergic neurons and synaptic dysfunctions, which may contribute to the autism-like behaviors by inducing excitatory/inhibitory imbalance.

Discussion

In this study, we integrated 26 DNVs in *GIGYF1* from a large cohort with 44,665 NDD trios, which includes 13,613 trios with a primary diagnosis of ASD and 31,052 trios with DD. We want to note that we included the majority of well-known cohorts that with underlying sequencing reads for reanalysis and/or detailed clinical records for phenotypic comparison, which should stand as a good representative set of NDD cohorts. We also

Author Manuscript Author Manuscript Author Manuscript Author Manuscript

want to note that the ASD and DD used and defined in this study refers to primary diagnosis, which means there maybe overlap of symptoms between ASD and DD, as it has been well-reported that differently diagnosed NDD patients are sometimes with overlapping phenotypes (25, 26). The patients carrying *GIGYF1* variants exhibit very similar phenotypes, strongly suggesting that variants in *GIGYF1* are probably the genetic causes of the disease. To further establish a causal relationship, we generated zebrafish and mouse models and demonstrated that loss of *Gigyf1* leads to developmental and behavioral defects that correlates with human phenotypes in both models.

In zebrafish mutants, the reduced body length in larval stage correlate with the global developmental delay in patients. The reduced interorbital distance and dysregulation of proliferation/apoptosis in zebrafish larvae are potentially corresponding to the microcephaly and dysmorphic face phenotypes. The behavioral phenotypes, including adaptation defects, elevated anxiety levels, reduced aggression and impaired social preference have all been widely considered as key features of ASD-related animal models that reflect the behavioral abnormalities in humans. The zebrafish model, thus, successfully recapitulates many aspects of the phenotypes of patients carrying loss-of-function mutations in *GIGYF1*.

We also systematically evaluated behavioral phenotypes in *Gigyf1* Het KO mice, *Gigyf1* e-cKO mice, and *Gigyf1* i-cKO mice, and detected convergent behavioral deficits including repetitive behaviors and social dysfunction. We found that deletion of *Gigyf1* in excitatory neurons increases repetitive behavior and impairs social memory, while loss of *Gigyf1* in inhibitory neurons increases anxiety level and impairs cognition. These findings in mice extend the observations in zebrafish, providing insights into the functions of *Gigyf1* in different neuronal subtypes. Previous studies showed that anxiety regulation is related to multiple brain regions, including medial prefrontal cortex (mPFC), lateral septum (LS), nucleus accumbens (NAc), central amygdala (CeA), basolateral amygdala (BLA), ventral tegmental area (VTA), and hippocampus (27). Some of these regions (i.e. LS, NAc, CeA) mainly include GABAergic neurons, while others include both excitatory and inhibitory neurons. Therefore, *Gigyf1* may regulate anxiety levels mainly through GABAergic neurons. It has been suggested that repetitive behaviors may be related to an imbalance of direct and indirect pathways in the basal ganglion (28–30). Notably, we detected elevated repetitive behavior in *Gigyf1* e-cKO mice, suggesting that *GIGYF1* in glutamatergic neurons may play a role in regulating the function of basal ganglion. Social behaviors are a series of social interactions between subject mouse and conspecifics, which involve continuous integration of multiple types of information including acute sensory inputs, internal social state, previous social experience retrieval and decision making(31). Here, we consistently observe a social memory deficit in both *Gigyf1* Het KO and *Gigyf1* e-cKO but not in *Gigyf1* i-cKO mice. It has been shown that hippocampal CA2 region and upstream inputs play crucial roles in social memory encoding (32–35). Here we detected an increased number of pyramidal neurons in hippocampal CA2 region. Moreover, the snRNAseq results also indicate the increased excitatory neuronal populations in the CA2 region. Therefore, the increased CA2 neurons may be responsible for the observed behavioral deficits.

One potential caveat is that NEX-Cre and GAD2-Cre mice may not have exactly the same genetic background, which may introduce some noise in neurobehavioral research (36). It

Author Manuscript Author Manuscript Author Manuscript Author Manuscript

has been shown that the brain weight, locomotor activity and ethanol preference in the same mouse strain were relatively stable in experiments performed in different labs across ~ 30 years (37). However, anxiety-related behaviors were highly variable across different labs, different times, and even different locations (37). Therefore, it is crucial to utilize littermate control and KO animals, which ensures the same sex, age, housing conditions as well as genetic background in neurobehavioral studies.

The second caveat is that distinct DNVs in *GIGYF1* observed in human patients may lead to early-stop, missense, or frameshift mutations, and each mutation may represent a unique subtype of *GIGYF1*-related neurodevelopmental disorders. Here we utilized *GIGYF1* KO zebrafish or mouse models, which may only mimic the loss-of-function mutations observed in human patients. It is highly possible that different *GIGYF1* DNVs may result in different structural and functional deficits, which are similar with other subtypes of *GIGYF1*-related disorders.

We also examined whether GIGYF1 is involved in gene regulation in the developing brain by transcriptomic and proteomic analyses. We identified more than a thousand potential targets of GIGYF1, many of which have been associated with different aspects of neurodevelopment and subtypes of NDDs (38, 39). Interestingly, in *GIGYF1* KO models of both species, synaptic protein expression was significantly disturbed (Figure 5F & G), suggesting an important role of *GIGYF1* in regulating synaptic functions.

In summary, our findings establish the relationship between variants in *GIGYF1* and neurodevelopmental defects, and help to establish the neuronal foundation for understanding the precise molecular mechanisms underlying clinical phenotypes related to *GIGYF1* loss-of-function mutations.

Supplementary Material

Refer to Web version on PubMed Central for supplementary material.

Acknowledgements

We thank Tonia Brown for assistance in editing this manuscript. We are grateful to the SPARK consortium for granting access to the exome sequencing data. This work is supported, in part, by grants from the National Natural Science Foundation of China (81671118, 81721005, 31871028 to B.X., 32271197 to M. J., and 82201314 to T.W.), by grants from the US National Institutes of Health (R01MH101221 and U01MH119705) and a grant from the Simons Foundation (SFARI #608045) to E.E.E., and by “the Fundamental Research Funds for the Central Universities” starting fund (BMU2022RCZX038) to T.W. E.E.E. is an investigator of the Howard Hughes Medical Institute. We acknowledge the support from the National Institute for Health Research through the Comprehensive Clinical Research Network.

References

1. Lai M-C, Lombardo MV, Baron-Cohen S (2014): Autism. The Lancet. 383:896–910.
2. Bernier R, Golzio C, Xiong B, Stessman HA, Coe BP, Penn O, et al. (2014): Disruptive CHD8 mutations define a subtype of autism early in development. Cell. 158:263–276. [PubMed: 24998929]
3. Stessman HA, Willemsen MH, Fenckova M, Penn O, Hoischen A, Xiong B, et al. (2016): Disruption of POGZ Is Associated with Intellectual Disability and Autism Spectrum Disorders. American journal of human genetics. 98:541–552. [PubMed: 26942287]

Author Manuscript Author Manuscript Author Manuscript Author Manuscript

4. Maenner MJ, Shaw KA, Baio J, EdS, Washington A, Patrick M, et al. (2020): Prevalence of Autism Spectrum Disorder Among Children Aged 8 Years - Autism and Developmental Disabilities Monitoring Network, 11 Sites, United States, 2016. MMWR Surveill Summ. 69:1–12.
5. X G, S L, L B, B W. (2018): Prevalence of Autism Spectrum Disorder Among US Children and Adolescents, 2014–2016. JAMA. 319:81–82. [PubMed: 29297068]
6. De Rubeis S, Buxbaum JD (2015): Genetics and genomics of autism spectrum disorder: embracing complexity. Human molecular genetics. 24:R24–31. [PubMed: 26188008]
7. Bai D, Yip BHK, Windham GC, Sourander A, Francis R, Yoffe R, et al. (2019): Association of Genetic and Environmental Factors With Autism in a 5-Country Cohort. JAMA psychiatry.
8. Iossifov I, O'Roak BJ, Sanders SJ, Ronemus M, Krumm N, Levy D, et al. (2014): The contribution of de novo coding mutations to autism spectrum disorder. Nature. 515:216–221. [PubMed: 25363768]
9. Ruzzo EK, Perez-Cano L, Jung JY, Wang LK, Kashef-Haghighi D, Hartl C, et al. (2019): Inherited and De Novo Genetic Risk for Autism Impacts Shared Networks. Cell. 178:850–866 e826. [PubMed: 31398340]
10. Turner TN, Coe BP, Dickel DE, Hoekzema K, Nelson BJ, Zody MC, et al. (2017): Genomic Patterns of De Novo Mutation in Simplex Autism. Cell. 171:710–722 e712. [PubMed: 28965761]
11. Krumm N, Turner TN, Baker C, Vives L, Mohajeri K, Witherspoon K, et al. (2015): Excess of rare, inherited truncating mutations in autism. Nature genetics. 47:582–588. [PubMed: 25961944]
12. Feliciano P, Zhou X, Astrovskaya I, Turner TN, Wang T, Brueggeman L, et al. (2019): Exome sequencing of 457 autism families recruited online provides evidence for autism risk genes. NPJ Genom Med. 4:19. [PubMed: 31452935]
13. Satterstrom FK, Kosmicki JA, Wang J, Breen MS, De Rubeis S, An JY, et al. (2020): Large-Scale Exome Sequencing Study Implicates Both Developmental and Functional Changes in the Neurobiology of Autism. Cell. 180:568–584 e523. [PubMed: 31981491]
14. Kaplanis J, Samocha KE, Wiel L, Zhang Z, Arvai KJ, Eberhardt RY, et al. (2020): Evidence for 28 genetic disorders discovered by combining healthcare and research data. Nature.
15. Giovannone B, Lee E, Laviola L, Giorgino F, Cleveland KA, Smith RJ (2003): Two novel proteins that are linked to insulin-like growth factor (IGF-I) receptors by the Grb10 adapter and modulate IGF-I signaling. The Journal of biological chemistry. 278:31564–31573. [PubMed: 12771153]
16. Amaya Ramirez CC, Hubbe P, Mandel N, Bethune J (2018): 4EHP-independent repression of endogenous mRNAs by the RNA-binding protein GIGYF2. Nucleic acids research.
17. Peter D, Weber R, Sandmeir F, Wohlbold L, Helms S, Bawankar P, et al. (2017): GIGYF1/2 proteins use auxiliary sequences to selectively bind to 4EHP and repress target mRNA expression. Genes & development. 31:1147–1161. [PubMed: 28698298]
18. Weber R, Chung MY, Keskeny C, Zinnall U, Landthaler M, Valkov E, et al. (2020): 4EHP and GIGYF1/2 Mediate Translation-Coupled Messenger RNA Decay. Cell Rep. 33:108262. [PubMed: 33053355]
19. Kim M, Semple I, Kim B, Kiers A, Nam S, Park HW, et al. (2015): Drosophila Gyf/GRB10 interacting GYF protein is an autophagy regulator that controls neuron and muscle homeostasis. Autophagy. 11:1358–1372. [PubMed: 26086452]
20. M CE, P FJ. (2019): An Accessible Protocol for the Generation of CRISPR-Cas9 Knockouts Using INDELs in Zebrafish. Methods in molecular biology. 1920:377–392. [PubMed: 30737704]
21. Zhou X, Feliciano P, Shu C, Wang T, Astrovskaya I, Hall JB, et al. (2022): Integrating de novo and inherited variants in 42,607 autism cases identifies mutations in new moderate-risk genes. Nature genetics. 54:1305–1319. [PubMed: 35982159]
22. Deciphering Developmental Disorders S (2017): Prevalence and architecture of de novo mutations in developmental disorders. Nature. 542:433–438. [PubMed: 28135719]
23. Wang T, Guo H, Xiong B, Stessman HAF, Wu H, Coe BP, et al. (2016): De novo genic mutations among a Chinese autism spectrum disorder cohort. Nature Communications. 7:13316.
24. Samocha KE, Robinson EB, Sanders SJ, Stevens C, Sabo A, McGrath LM, et al. (2014): A framework for the interpretation of de novo mutation in human disease. Nature genetics. 46:944–950. [PubMed: 25086666]

Author Manuscript Author Manuscript Author Manuscript Author Manuscript

25. Matson JL, Shoemaker M (2009): Intellectual disability and its relationship to autism spectrum disorders. Res Dev Disabil. 30:1107–1114. [PubMed: 19604668]
26. Wang T, Kim CN, Bakken TE, Gillentine MA, Henning B, Mao Y, et al. (2022): Integrated gene analyses of de novo variants from 46,612 trios with autism and developmental disorders. Proc Natl Acad Sci U S A. 119:e2203491119.
27. Calhoon GG, Tye KM (2015): Resolving the neural circuits of anxiety. Nat Neurosci. 18:1394–1404. [PubMed: 26404714]
28. DiCarlo GE, Aguilar JI, Matthies HJ, Harrison FE, Bundschuh KE, West A, et al. (2019): Autism-linked dopamine transporter mutation alters striatal dopamine neurotransmission and dopamine-dependent behaviors. J Clin Invest. 129:3407–3419. [PubMed: 31094705]
29. Paval D (2017): A Dopamine Hypothesis of Autism Spectrum Disorder. Dev Neurosci. 39:355–360. [PubMed: 28750400]
30. Tecuapetla F, Matias S, Dugue GP, Mainen ZF, Costa RM (2014): Balanced activity in basal ganglia projection pathways is critical for contraversive movements. Nat Commun. 5:4315. [PubMed: 25002180]
31. Chen P, Hong W (2018): Neural Circuit Mechanisms of Social Behavior. Neuron. 98:16–30. [PubMed: 29621486]
32. Hitti FL, Siegelbaum SA (2014): The hippocampal CA2 region is essential for social memory. Nature. 508:88–92. [PubMed: 24572357]
33. Oliva A, Fernandez-Ruiz A, Leroy F, Siegelbaum SA (2020): Hippocampal CA2 sharp-wave ripples reactivate and promote social memory. Nature. 587:264–269. [PubMed: 32968277]
34. Pimpinella D, Mastrorilli V, Giorgi C, Coemans S, Lecca S, Lalive AL, et al. (2021): Septal cholinergic input to CA2 hippocampal region controls social novelty discrimination via nicotinic receptor-mediated disinhibition. Elife. 10:e65580. [PubMed: 34696824]
35. Wu X, Morishita W, Beier KT, Heifets BD, Malenka RC (2021): 5-HT modulation of a medial septal circuit tunes social memory stability. Nature. 599:96–101. [PubMed: 34616037]
36. Matsuo N, Takao K, Nakanishi K, Yamasaki N, Tanda K, Miyakawa T (2010): Behavioral profiles of three C57BL/6 substrains. Front Behav Neurosci. 4:29. [PubMed: 20676234]
37. Wahlsten D, Bachmanov A, Finn DA, Crabbe JC (2006): Stability of inbred mouse strain differences in behavior and brain size between laboratories and across decades. Proc Natl Acad Sci U S A. 103:16364–16369. [PubMed: 17053075]
38. Li X, Zhang K, He X, Zhou J, Jin C, Shen L, et al. (2021): Structural, Functional, and Molecular Imaging of Autism Spectrum Disorder. Neuroscience Bulletin. 37:1051–1071. [PubMed: 33779890]
39. Parenti I, Rabaneda LG, Schoen H, Novarino G (2020): Neurodevelopmental Disorders: From Genetics to Functional Pathways. Trends Neurosci. 43:608–621. [PubMed: 32507511]

Author Manuscript Author Manuscript Author Manuscript Author Manuscript

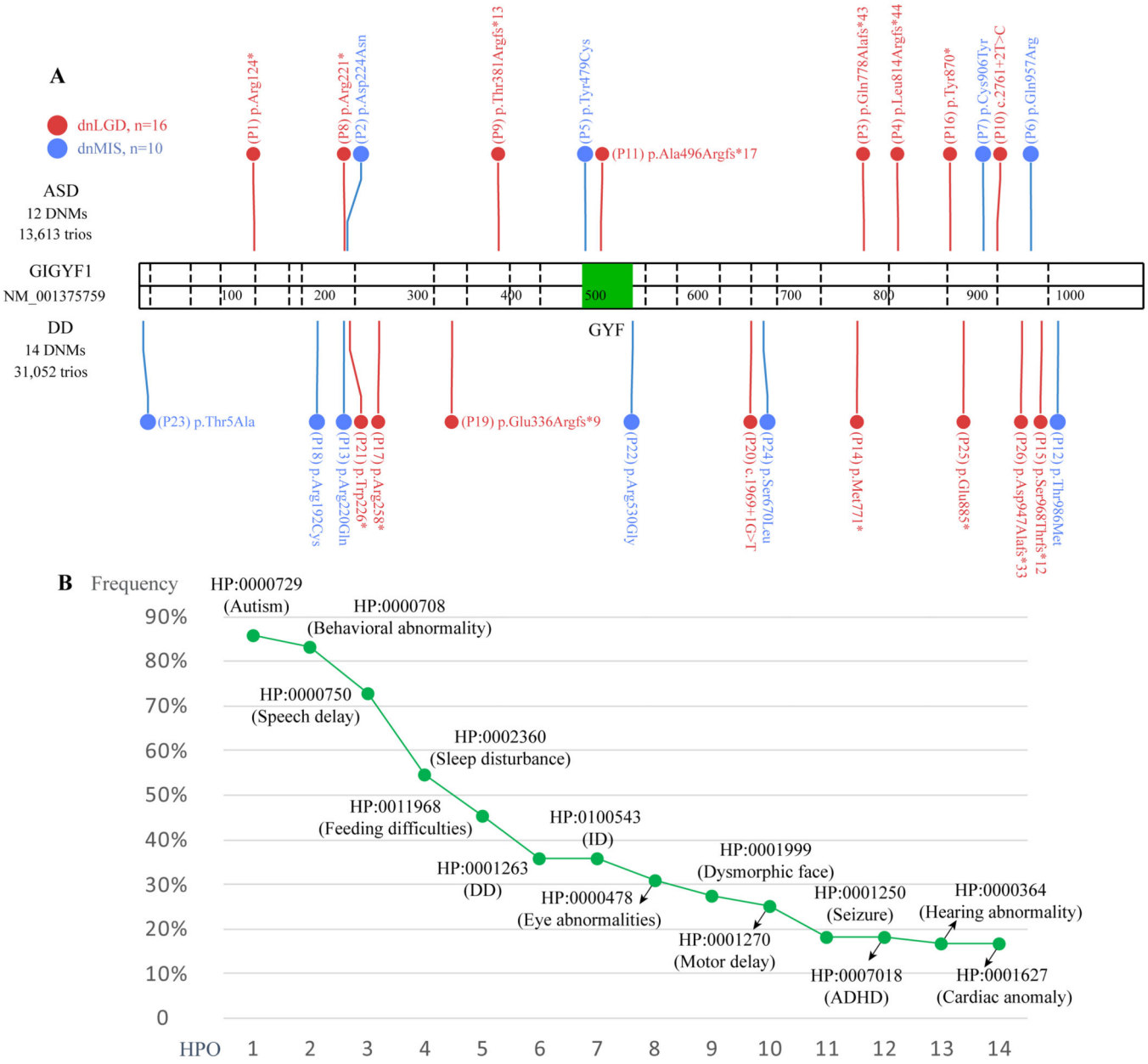

Figure 1. *De novo* variants in *GIGYF1* and the HPO frequencies.

A, dnLGD (red) and dnMIS (blue) variants in ASD (above) and DD (below) cohorts are depicted against a protein diagram for GIGYF1, the ASD and DD defined in this study refers to the primary diagnosis. GYF: domain contains conserved Gly-Tyr-Phe residues (middle green block). **B,** The HPO phenotype frequencies were calculated only among the patients with phenotypic information available, phenotypes with description available for less than 10 individuals were excluded from the calculation.

Author Manuscript Author Manuscript Author Manuscript Author Manuscript

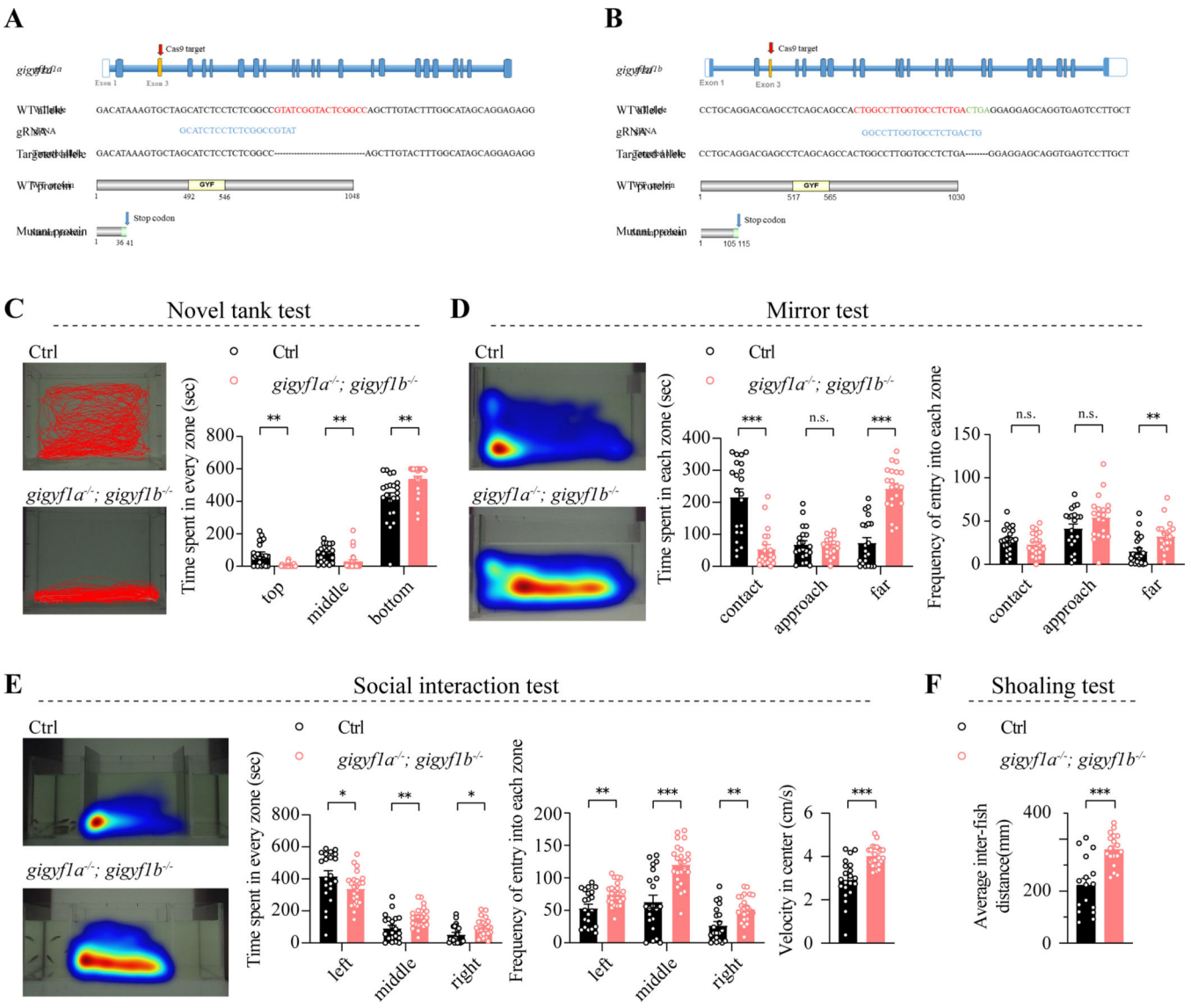

Figure 2. Knockout of zebrafish homologs of *GIGYF1* causes various behavioral defects.

A, B, Strategies for generating zebrafish *gigyf1a* and *gigyf1b* knockout alleles using the CRISPR/Cas9 system, respectively. An allele with a 16 bp deletion in exon 3 of *gigyf1a*, and an allele with a 4 bp deletion for *gigyf1b* were isolated. These alleles all cause frameshift and early truncation for the proteins. Double mutant allele *gigyf1a*$^{-/-}$; *gigyf1b*$^{-/-}$ was then generated by crossing the single mutants. **C,** In the novel tank test, *gigyf1a*$^{-/-}$; *gigyf1b*$^{-/-}$ mutants spent significantly reduced time in the top region and prolonged time in the bottom region. **D,** In the mirror test, *gigyf1a*$^{-/-}$; *gigyf1b*$^{-/-}$ mutants were further away from the mirror compare to the controls. **E,** In the social interaction test, *gigyf1a*$^{-/-}$; *gigyf1b*$^{-/-}$ mutants exhibited reduced interest to the left chamber where other fishes were trapped. **F,** The average distance between the *gigyf1a*$^{-/-}$; *gigyf1b*$^{-/-}$ mutants was greater than that of the controls in the shoaling test. Data in summary graphs are means ± SEM; statistical comparisons were performed with student's t-test (n.s. $p > 0.05$; *, $p < 0.05$; **, $p < 0.01$; ***, $p < 0.001$).

Author Manuscript Author Manuscript Author Manuscript Author Manuscript

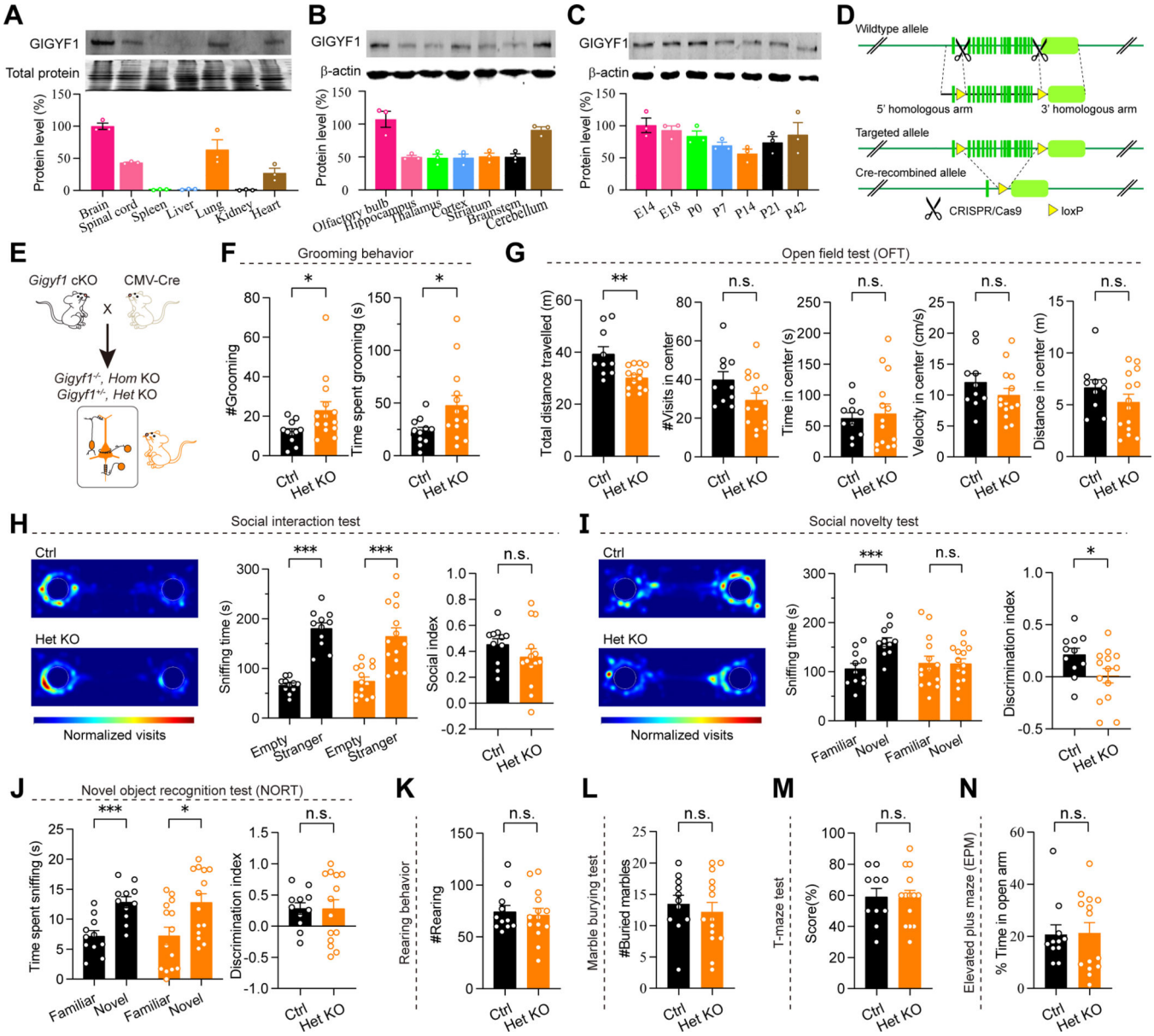

Figure 3: Haploinsufficiency of *Gigyf1* causes excessive repetitive behavior and impaired social memory.

A, Western blot analysis of Gigyf1 protein levels in mouse brain, spinal cord, spleen, liver, lung, kidney and heart at postnatal day 42 (P42). Total protein was used as an internal control (n = 3). **B,** Western blot analysis of *GIGYF1* protein levels in the different brain regions (n = 3). **C,** *GIGYF1* protein levels in the developing mouse brain determined by western blot (n = 3). **D,** Targeting strategy for the generation of conditional *Gigyf1* KO mice in which 10th −24th exons were conditionally deleted by Cre recombinase. **E,** *Gigyf1* is deleted by crossing *Gigyf1* cKO mice with CMV-cre mice. **F,** The grooming bouts and duration are analyzed in control and *Gigyf1* Het KO mice, respectively (p = 0.0394 and 0.0353; control, n = 11; Het, n = 14). **G,** Open filed test (OFT) reveals a reduced locomotion in *Gigyf1* Het KO mice (p = 0.0031; control, n = 11; Het, n = 14). **H,** During social

Author Manuscript Author Manuscript Author Manuscript Author Manuscript

interaction session, *Gigyf1* Het KO mice have normal sociability. Left, position heat maps for the control and Het mice. Middle, the sniffing time. Right, social index ($p > 0.05$; control, n = 11; Het, n = 14). **I,** The same as panel H but for social novelty test. Left, position heat maps. Middle, the sniffing time exploring S1 and S2. Right, social discrimination index ($p = 0.0246$; control, n = 11; Het, n = 14). **J,** *Gigyf1* Het KO mice exhibit a normal recognition level in the novel object recognition test (NORT) ($p > 0.05$; control, n = 11; Het, n = 14). **K,** Rearing behavior. **L,** Marble burying test. **M,** T-maze test. **N,** Elevated plus maze. Data in summary graphs are means ± SEM; statistical comparisons were performed with student's t-test (n.s. $p > 0.05$; *, $p < 0.05$; **, $p < 0.01$; ***, $p < 0.001$).

Author Manuscript Author Manuscript Author Manuscript Author Manuscript

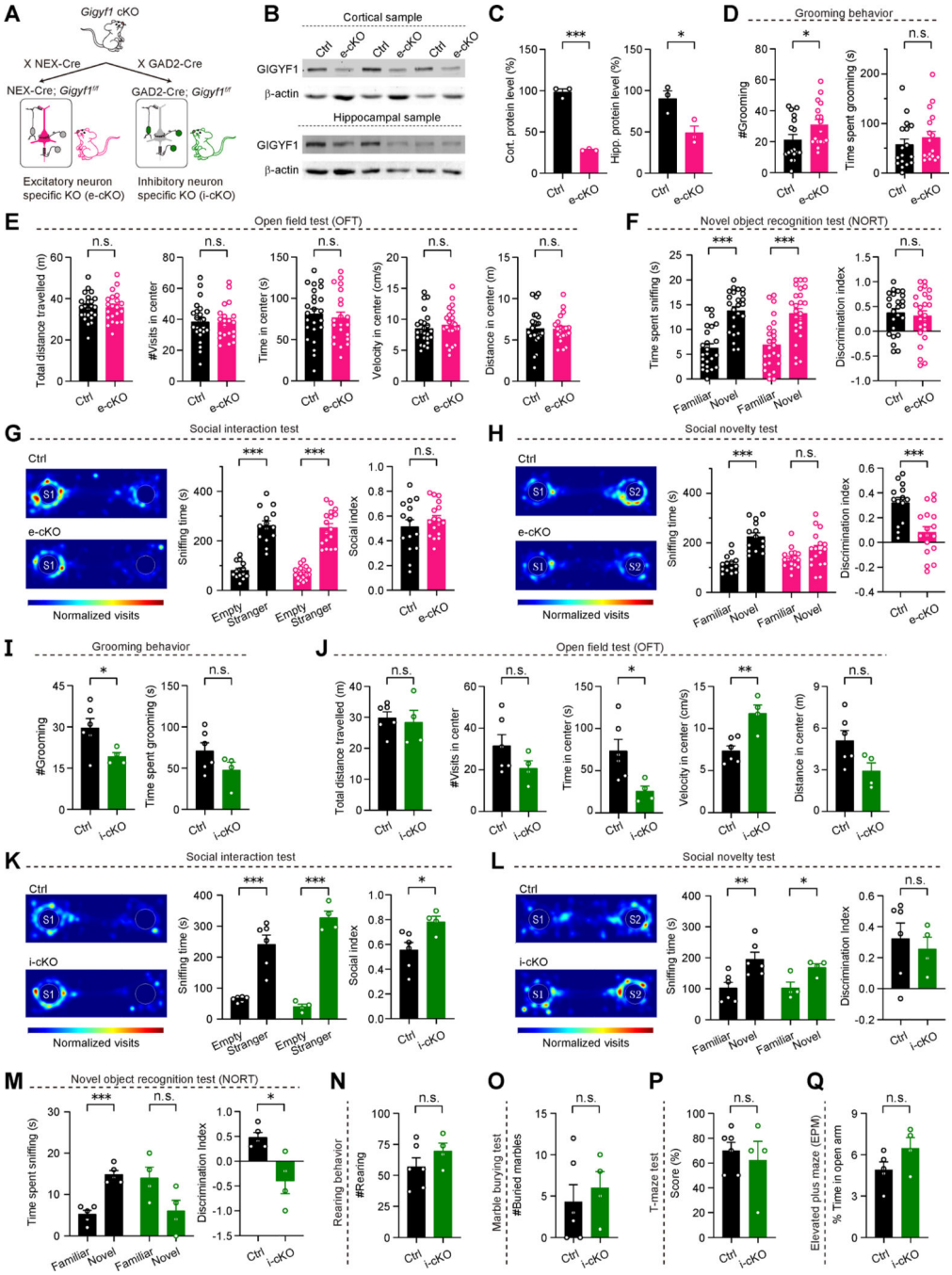

Figure 4: Deletion of *Gigyf1* in excitatory neurons and inhibitory neurons results in differential behavioral deficits in repetitive behavior, social memory, anxiety and cognition.

A, *Gigyf1* is conditionally deleted in excitatory neurons (*Gigyf1* e-cKO) and inhibitory neurons (*Gigyf1* i-cKO), respectively. **B,** Western blots of cortical (left) and hippocampal (right) lysate from control and *Gigyf1* e-cKO mice. **C,** Summary graphs showing that *GIGYF1* protein levels are decreased in *Gigyf1* e-cKO mice (cortical KO = 31.86 ± 0.81%, n = 3, p<0.001; hippocampal KO = 55.87 ± 6.464%, n = 3, p = 0.003), and all the values are normalized and compared to the WT. **D,** The grooming bouts and duration are analyzed

Author Manuscript Author Manuscript Author Manuscript Author Manuscript

in *Gigyf1* e-cKO, respectively (p = 0.0496 and 0.4066; control, n = 17; e-cKO, n = 17). **E,** Open filed test (OFT) suggests anxiety level is not changed in *Gigyf1* e-cKO mice (p > 0.05; control, n = 24; e-cKO, n = 21). **F,** *Gigyf1* e-cKO mice exhibit a normal recognition level in the novel object recognition test (NORT) (p>0.05; control, n = 24; e-cKO, n = 25). **G,** during social interaction session, *Gigyf1* e-cKO mice have normal sociability. Left, position heat maps for the control and *Gigyf1* e-cKO mice exploring the pencil cups with or without stranger 1 (S1). Middle, the sniffing time the subject mice spent in the circle (20 cm in diameter) surrounding the pencil cup which is empty or has a stranger (S1) in it. Right, social index (p > 0.05; control, n = 14; e-cKO, n = 17). **H,** the same as panel G but for social novelty test. Left, position heat maps. Middle, the sniffing time exploring stranger 1 (familiar stranger S1) and stranger 2 (novel stranger S2). Right, social discrimination index (p = 0.0009; control, n = 14; e-cKO, n = 17).

I, The grooming bouts and duration are analyzed in *Gigyf1* i-cKO, respectively (p = 0.0451 and 0.1522; control, n = 6; i-cKO, n = 4). **J,** Open filed test (OFT) suggests anxiety level is elevated in *Gigyf1* i-cKO mice (p > 0.05; control, n = 6; i-cKO, n = 4).

K, During social interaction session, *Gigyf1* i-cKO mice have normal sociability. Left, position heat maps for the control and *Gigyf1* i-cKO mice. Middle, the sniffing time. Right, social index (p > 0.05; control, n = 6; i-cKO, n = 4). **L,** The same as panel **K** but for social novelty test. Left, position heat maps. Middle, the sniffing time exploring S1 and S2. Right, social discrimination index (p > 0.05; control, n = 6; i-cKO, n = 4). **M,** *Gigyf1* i-cKO mice exhibit impaired recognition level in the novel object recognition test (NORT) (p = 0.0101; control, n = 5; i-cKO, n = 4). **N,** Rearing behavior. **O,** Marble burying test. **P,** T-maze test. **Q,** Elevated plus maze. Data in summary graphs are means ± SEM; statistical comparisons were performed with student's t-test (n.s. p > 0.05; *, p < 0.05; **, p < 0.01; ***, p < 0.001).

Author Manuscript Author Manuscript Author Manuscript Author Manuscript

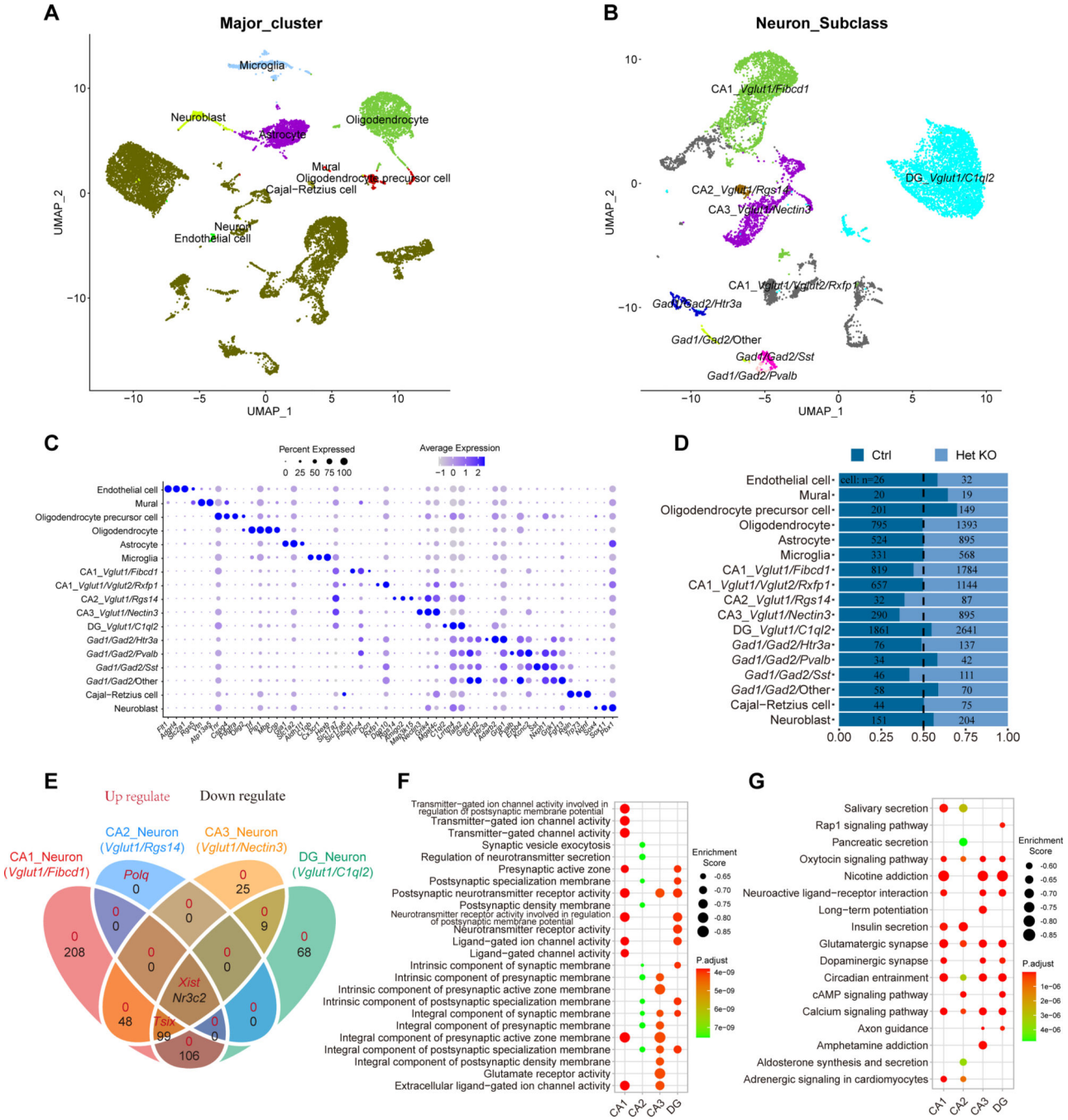

Figure 5: Single-nuclei RNA sequencing of hippocampus from P42 *Gigyf1* Het KO mice

A. Uniform manifold approximation and projection (UMAP) of hippocampal cells of *Gigyf1* Het KO and Control mice, which were clustered into 9 major cell types. **B.** The hippocampal neurons from *Gigyf1* Het KO and Control mice were clustered into nine neuronal subpopulations, including five classes of excitatory neurons and four classes of inhibitory neurons. **C.** Dot plots showing molecular signatures of clusters from a and b. The percentage of cells expressing the gene (circle size) and average gene expression level (colour scale) were displayed. **D.** Relative proportions and number of cells in the clusters

Author Manuscript Author Manuscript Author Manuscript Author Manuscript

between the *Gigyf1* Het KO and control samples. **E.** The intersections of DEGs among clusters of CA1_*Vglut1/Fibcd1*, CA2_*Vglut1/Rgs14*, CA3_*Vglut1/Nectin3* and DG_*Vglut1/C1ql2*. Differential expression analyses were performed between the *Gigyf1* Het KO and the Ctrl group (up-regulated genes in red and down-regulated genes in black). **F.** GSEA of CA1_*Vglut1/Fibcd1*, CA2_*Vglut1/*Rgs14, CA3_*Vglut1/Nectin3* and DG_*Vglut1/C1ql2* clusters based on the GENE ONTOLOGY database. **G.** GSEA of CA1_*Vglut1/Fibcd1*, CA2_*Vglut1/Rgs14*, CA3_*Vglut1/Nectin3* and DG_*Vglut1/C1ql2* clusters based on the KEGG PATHWAY database.

Author Manuscript Author Manuscript Author Manuscript Author Manuscript

KEY RESOURCES TABLE

Resource Type	Specific Reagent or Resource	Source or Reference	Identifiers	Additional Information
Add additional rows as needed for each resource type	Include species and sex when applicable.	Include name of manufacturer, company, repository, individual, or research lab. Include PMID or DOI for references; use “this paper” if new.	Include catalog numbers, stock numbers, database IDs or accession numbers, and/or RRIDs. RRIDs are highly encouraged; search for RRIDs at https://scicrunch.org/resources.	Include any additional information or notes if necessary.
Antibody	rabbit anti-GIGYF1	Sigma-Aldrich	HPA023995	
Antibody	rabbit anti-β-actin	Proteintech	20536–1-AP	
Antibody	mouse anti-GAPDH	Proteintech	60004–1-Ig	
Antibody	rabbit anti- NeuN	Abcam	ab177487	
Antibody	rabbit anti-VGLUT2	Sigma-Aldrich	V2514	
Antibody	rabbit anti-GAD65/67	Sigma-Aldrich	G5163	
Antibody	rabbit anti-Phospho-Histone H3 (Ser10)	CellSignalingTechnology	3377S	
Antibody	Alexa Fluor™ 488 conjugated goat anti-rabbit secondary antibody	ThermoFisher Scientific	A11034	
Antibody	Alexa Fluor™ 800 conjugated goat anti-rabbit secondary antibody	ThermoFisher Scientific	A32735	
Antibody	Alexa Fluor™ 800 conjugated goat anti-mouse secondary antibody	ThermoFisher Scientific	A32730	
Chemical Compound or Drug	T7 RNA polymerase	Roche	10881767001	
Chemical Compound or Drug	DIG RNA Labeling Mix	Roche	11277073910	
Chemical Compound or Drug	TRIzol™ Reagent	ThermoFisher Scientific	15596026	
Chemical Compound or Drug	ChamQ SYBR qPCR Master Mix	Vazyme	Q311–02	
Chemical Compound or Drug	RIPA Lysis Buffer I	Sangon Biotech	C500005	
Chemical Compound or Drug	Protease Inhibitor Cocktail	MedChemExpress	HY-K0010	
Commercial Assay Or Kit	mMESSAGE mMACHINE® T3 Kit	ThermoFisher Scientific	AM1348	
Commercial Assay Or Kit	Maxima™ H Minus First Strand cDNA Synthesis Kit	ThermoFisher Scientific	K1652	
Commercial Assay Or Kit	Revert™ 700 Total Protein Stain Kits	LI-COR Biosciences	P/N 926–11010	
Commercial Assay Or Kit	Micro-BCA Protein Assay Kit	Sangon Biotech	C503061	
Commercial Assay Or Kit	HiScript III RT SuperMix	Vazyme	R323–01	

Author Manuscript Author Manuscript Author Manuscript Author Manuscript

Resource Type	Specific Reagent or Resource	Source or Reference	Identifiers	Additional Information
Commercial Assay Or Kit	NEBNext® Ultra™ II RNA Library Prep Kit for Illumina®	New England Biolabs	E7770S	
Commercial Assay Or Kit	TruSeq PE Cluster Kit v3-cBot-HS	Illumina	PE-401–3001	
Commercial Assay Or Kit	Chromium Nuclei Isolation Kit with RNase Inhibitor	10x Genomics	PN-1000494	
Commercial Assay Or Kit	Chromium Next GEM Single Cell 3′ GEM, Library & Gel Bead Kit v3.1	10x Genomics	PN-1000121	
Deposited Data; Public Database	Human Phenotype Ontology	Monarch Initiative	RRID:SCR_006016	
Deposited Data; Public Database	Mouse Brain Atlas	Linnarsson Lab	RRID:SCR_018356	
Deposited Data; Public Database	DropViz	McCarroll Lab	http://dropviz.org/	
Deposited Data; Public Database	Allen Cell Types Database	Allen Institute	RRID:SCR_014806	
Deposited Data; Public Database	SFARI Gene database	Simons Foundation	RRID:SCR_004261	
Deposited Data; Public Database	Deciphering Developmental Disorders Gene database	PMID: 19344873	RRID:SCR_006171	
Deposited Data; Public Database	DisGeNET database	PMID: 34136095	RRID:SCR_006178	
Organism/Strain	Zebrafish:Tuebingen	China Zebrafish Resource Center	CZRC Catalog ID: CZ3	
Recombinant DNA	pT3TS(T3:zCas9-UTRglobin)	China Zebrafish Resource Center	CZRC Catalog ID: CZP11	
Software; Algorithm	GATK	PMID: 20644199	RRID:SCR_001876	
Software; Algorithm	FreeBayes	https://doi.org/10.48550/arXiv.1207.3907	RRID:SCR_010761	
Software; Algorithm	Variant Effect Predictor	PMID: 27268795	RRID:SCR_007931	
Software; Algorithm	Combined Annotation Dependent Depletion	PMID: 33618777	RRID:SCR_018393	
Software; Algorithm	EthoVision XT7	Noldus	RRID:SCR_000441	
Software; Algorithm	DESeq2 R package	PMID: 25516281	RRID:SCR_015687	
Software; Algorithm	clusterProfiler R package	PMID: 34557778	RRID:SCR_016884	
Software; Algorithm	Viewer III	Biobserve	RRID:SCR_014337	
Software; Algorithm	FreezeFrame	Colbourn Instruments	RRID:SCR_014429	
Software; Algorithm	Cell Ranger v7.0.1	10x Genomics	RRID:SCR_017344	
Software; Algorithm	Seurat R package	PMID: 34062119	RRID:SCR_016341	
Software; Algorithm	DoubletFinder R package	PMID: 30954475	RRID:SCR_018771	
Software; Algorithm	Harmony R package	PMID: 31740819	RRID:SCR_022206	
Software; Algorithm	Monocle2 R package	PMID: 28114287	RRID:SCR_016339	